ISSN: 2795-2215

Journal of Newviews in Engineering & Technology
Faculty of Engineering
Rivers State University, Port Harcourt, Nigeria.

Email: rsujnet@gmail.com | Homepage:www.rsujnet.org

Added Resistance and Seakeeping Analyses of a Very Large Crude-Oil Carrier in the Gulf of Guinea

Abali, E. D.*, Samson, N., Azubuike, J. C.

Department of Marine Engineering, Rivers State University, PMB 5080 Port Harcourt, Nigeria.

**Corresponding Author: datonyeabali@icloud.com*

ARTICLE INFO

Article History
Received: 22 August 2024
Received in revised form: 27 October 2024
Accepted: 27 October 2014
Available online: 18 December 2024

Keywords
Marine Engineering; Naval Architecture; Response Amplitude; Total Ship Resistance; Vessel Drafts

ABSTRACT

Very Large Crude-Oil Carriers (VLCCs) often operate outside design conditions, affecting energy efficiency and emissions. This study investigated the impact of waves on added resistance and seakeeping of VLCCs in the Gulf of Guinea. Using numerical simulations, we evaluated added resistance for speeds between 10-14 knots under varying wave periods and vessel drafts. The study also analyzed Response Amplitude Operators (RAOs) for heave, roll, and pitch motions; and identified critical frequencies. Results showed up to a 30% reduction in resistance at higher speeds. Moreover, the RAOs analysis provided valuable insights for optimizing VLCC operations, balancing fuel efficiency, risk assessment, and safety. These findings may inform route planning, vessel design, and emission reduction strategies.

1. Introduction

As a ship moves through calm water, it experiences a force acting opposite to its direction. This force is the water's resistance to the motion of the ship, known as the total resistance. Until the early 1860s, very little was understood about ship resistance, and the visions of powering were unreliable. Design was centered on trial and error, and the wrong prime movers were installed resulting in low-cost effectiveness and an increase in time wastage. These loopholes indicated a necessity in the development of predictive methods for the early stages of ship design and main engine selection (Petersson, 2002). The optimization of the preceding methods can be achieved with the use of the comprehensive naval architecture software, Maxsurf. Its integrated tools allow the modelling and performance evaluation of hull structures, offshore platforms, and vessels in general.

The investigation into the seakeeping of ships encompasses several critical issues. These include the maximum speed in a seaway, which involves both involuntary speed reductions due to increased resistance from waves and conscious reductions to prevent excessive motions and loads (ITTC, 2017). Route optimization is also a key consideration, aimed at enhancing fuel efficiency, reducing transport time, and

minimizing total costs. Habitation comfort and safety for individuals on board are paramount, addressing concerns such as motion sickness, the risk of accidental falls, and man overboard incidents. Finally, ship safety is a major focus, with attention to risks like capsizing, large roll motions and accelerations, slamming from wave impacts on superstructures or deck cargo, and propeller racing that can lead to excessive engine rotation per minutes (Bertram, 2011). As hydrodynamic theories have continued to be revised for the improvement of ship performance, the existence and utilization of database paves a way for more accurate estimations of the total resistance and overall performance of a ship.

In calm water, the wave resistance occurs as a result of the wave-making and wave-breaking resistances, as well spray generation. Nitonye & Adumene (2015) researched on a 25,000 DWT tanker vessel involving five model speeds, which had their equivalent ship speeds in accordance with Froude's law of similitude. The results showed a progression in resistance with higher wave formation, and a variation in bare-hull resistance at different model speeds. In waves, the ship experiences an increase in resistance due to actual waves known as added wave resistance (Roser, 2018). Added resistance becomes more prominent as the wave length approaches the ship length. In a numerical analysis of a container vessel with wave length to ship length ranging from 05 to 2.0 times the ship's length. el Moctar et al., (2017) results showed that at a Froude number of 0.28, the added resistance in short waves was relatively low, while in longer waves, added resistance reached its peak. Seo et al. (2017) conducted a study to examine the effects of wave periods on the added resistance and motion characteristics of a 3600 TEU KRISO Container Ship (KCS) in head sea conditions. The study utilized computational fluid dynamics, specifically the OpenFOAM software, to simulate the ship's behaviour in various wave scenarios. These simulations allowed for the examination of how varying wave periods influenced both the added resistance and the heave and pitch motions of the ship. The study's findings highlighted a significant increase in added resistance when the wave length approached the length of the ship, and the heave and pitch motions were most significantly amplified when the wave length was approximately 1.15 to 1.55 times the ship's length. Following a study on Nawigator XXI, Niklas & Karczewski (2020) provided valuable insights into the general seakeeping performance and added resistance of vessels using the strip method. The analysis highlights that the vessel's performance in head waves was influenced by its speed and wave conditions, with added resistance increasing significantly as wave height and speed increased. At moderate speeds, the vessel experienced moderate levels of pitching and heaving, but these motion amplitudes increased considerably in longer waves, impacting overall seakeeping performance. The heave RAO for the vessel showed a peak value of approximately 0.42 meters in longer waves and 0.12 meters for shorter waves. Pitch RAO reached a peak of 2.22 degrees for longer waves and 0.75 degrees for shorter waves. Additionally, added resistance varied significantly depending on wave period and vessel speed, with values reaching 18.54kN in longer waves and 3.19kN in shorter waves, demonstrating that added resistance increases substantially in rougher sea conditions, affecting vessel performance and fuel efficiency.

Ibinabo & Tamunodukobipi (2019) study on the determination of RAOs provided valuable insights into seaworthiness of a Floating Production Storage and Offloading (FPSO) vessel. In the study, a numerical simulation tool was utilized to compute

RAOs for all six degrees of freedom including surge, sway, heave, roll, pitch, and yaw. Specifically, it was found that the heave motion RAO tends to increase towards higher encounter frequencies when the wave direction was changed from a head sea to a beam sea. The key finding from the study was the variation in heave RAO with changing wave headings, particularly the shift towards higher frequencies as the wave direction moved from head to beam seas. For a VLCC, understanding these shifts is critical for optimizing its design and operation in regions like the Gulf of Guinea, where varying wave headings could impact both its seakeeping performance and the added resistance it faces.

Mazzaretto et al. (2022) examined the suitability of the standard JONSWAP peak-enhancement factor (γ = 3.3) in coastal regions worldwide. The study found that the actual value varied significantly across different coastal areas, often being lower than the standard value, particularly along eastern continental coasts, where γ was commonly below 2.4. The study concluded that although the standard JONSWAP formulation may not always accurately represent local wave conditions, the standard value provides a reasonable approximation for many offshore conditions.

Yan et al. (2018) studied the influence of various wave spectra on the motion responses of a dynamically positioned ship. The results of the study suggest that the JONSWAP spectrum produces more controlled motion amplitudes, especially in surge, making it effective in predicting ship responses in wave-induced scenarios. Taskar & Andersen (2021) explored different methods for calculating added resistance in waves, focusing on the JONSWAP spectrum. The study suggests that while the choice of γ in the JONSWAP spectrum may not drastically alter the results, it becomes more relevant in high sea states, where added resistance plays a crucial role in overall vessel performance.

The Gulf of Guinea is a crucial maritime region, known for its heavy shipping traffic and complex wave patterns, which significantly impact the operations of large vessels. Despite its importance, there is limited research focusing on the specific challenges posed by the wave conditions in this region, particularly concerning the added resistance and seakeeping performance of VLCCs. The lack of region-specific research for the Gulf of Guinea means that many of the assumptions and models used do not accurately reflect the actual conditions and are less reliable. Addressing these problems requires a focused investigation into the influence of predominant wave headings in the Gulf of Guinea on the added resistance and seakeeping performance of VLCCs. Also, without a thorough understanding of how wave heading influences seakeeping, there is an increased risk of accidents, such as cargo shifting, structural damage, or even capsizing in extreme cases (Zu et al., 2024). This study analyzed the added resistance and seakeeping of a tanker vessel to add more insight to the existing investigations in ship resistance and propulsion, particularly in the Gulf of Guinea region. This, in turn, will lead to improved safety, cost efficiency, and environmental sustainability in VLCC operations.

2. Materials and Methods

2.1 Materials

Materials used in this study include (but not limited to) Bentley's MAXSURF modules, Microsoft Excel, data from Bonga Metocean Reference Document (MRD), and a personal computer.

2.2 Methods

The main particulars of the ship and model are shown in Table 1. The hindcast data from a Bonga

MRD was filtered to extract the prevalent wave height of 1.49m specific to the Gulf of Guinea, along with its associated wave periods. This approach ensured that the selected wave parameters accurately reflect the most frequent sea state of the region, providing a realistic basis for evaluating the added resistance and seakeeping performance of the vessel. With a peak enhancement factor (PEF) of 3.3, the JONSWAP spectrum is selected to illustrate the energy distribution and identify the critical frequencies that the VLCC would respond to.

Table 1: Parameters of Very Large Crude-Oil Carrier.

Parameter	Value
L_{OA} (m)	332.8
L_{WL}(m)	325.5
L_{BP} (m)	320.0
Beam, B (m)	60
Depth, D (m)	30
Draft, T (m)	20
Block Coefficient, CB	0.8098

Source: Ouargli & Hamoudi (2021).

2.2.1 Calm Water Resistance Analysis

Resistance components, including frictional resistance, wave resistance, air resistance, etc. were assembled into the total resistance in equation 1.

$$R_T = (1+k)R_F + R_W \quad (1)$$

Where k = Form Factor; R_F = Frictional Resistance; and R_W = Wave Resistance. Frictional Resistance, R_F, is given by equation 2.

$$\mathrm{R_F} = \frac{1}{2}\rho V_s^2 \mathrm{S C_F} \quad (2)$$

$$\mathrm{C_F} = \frac{0.075}{[\log_{10}(\mathrm{R_e})-2]^2} \quad (3)$$

$$\mathrm{S} = \mathrm{C_{23}L_{WL}(2T+B)}\sqrt{\mathrm{C_M}} + 2.38\frac{\mathrm{A_{BT}}}{\mathrm{C_B}} \quad (4)$$

Where, L_{WL} = Waterline length, T = draft, B = Beam; A_{BT} = Transverse Area of Bulbous Bow, C_B = Block Coefficient, and $\mathrm{C_M} = \frac{\mathrm{C_B}}{\mathrm{C_P}} =$ Midship Section Coefficient.

According to Birk (2019), the wave resistance for Froude numbers, $F_r < 0.4$ is represented as shown in equation 5.

$$\mathrm{R_{Wa}(F_r)} = \mathrm{C_1C_2C_5\rho_g V \exp\,[m_1 F_{r^d} + m_4 \cos(\lambda F_{r^{-2}})]} \quad (5)$$

Where C_1, C_2, C_5, λ, m_1, m_4, and d are additional coefficients for the wave resistance computation with their respective criteria.

2.2.2 Added Resistance and Seakeeping Analyses due to Wave Forces

The analyses for both added resistance and seakeeping are based on complex equations too cumbersome to be solved manually. Strip theory is applied in the MAXSURF motions to analyze the influence of waves on the VLCC. It relies on linear wave theory, boundary conditions for the hull and free surface, as well as hydrodynamic forces. Linear wave theory assumes small amplitude waves and linear superposition. The wave potential, $\emptyset$, is given by equation 6.

$$\emptyset(r,t) = \Re[\emptyset(x,y,\omega)e^{-i(kx-\omega t}] \quad (6)$$

Where, $\emptyset$ = Wave potential, $\emptyset(x,y,\omega)$ = Complex amplitude of the wave potential, ω = Angular frequency, r = Position vector, and t = Time.

Hydrodynamic forces acting on the VLCC determine how the ship would respond in terms of pitch and heave motions governed by the equation of motion, equation 7, with the wave force expressed in equation 8 calculated using potential flow theory.

$$m\dot{z} + c\dot{z} + k\dot{z} = F_x \quad (7)$$

Where $m =$ Mass of the strip, $c =$ Damping Coefficient, $k =$ Stiffness coefficient, $\dot{z} =$displacement of the strip.

$$F_x(x,t) = \frac{\partial(\rho\left(\frac{\partial\emptyset}{\partial z}\right)}{\partial x} \quad (8)$$

When applying linear strip theory, the wave conditions are characterized using the JONSWAP spectrum expressed in equation (9). The spectrum provides the formulation of long-crested wave formulation and the necessary input for defining the wave field's energy distribution Bai & Bai (2005). Linear strip theory then uses this wave spectrum to predict how a ship or structure will respond to these waves.

$$S(\omega) = \frac{\alpha g^2}{\omega^4}\, exp\left(-\frac{1}{2}\left(\frac{\omega}{\omega_p}\right)^{-4}\right) \times \gamma^{exp\left(-\frac{(\omega-\omega_p)^2}{2\sigma^2\omega_P{}^2}\right)} \quad (9)$$

Where $\omega = 2\pi f$ (f is the frequency), $\omega_p =$ Peak angular frequency, $\alpha =$ Phillip's constant, which is related to the wave energy, $g =$ Acceleration due to gravity, $\gamma =$ Peak enhancement factor (usually greater than 1), which indicates the sharpness of the spectrum's peak, $\sigma =$ A parameter that defines the width of the peak in the frequency domain (typically, 0.07 for $\omega < \omega_p$ and 0.09 for $\omega \geq \omega_p$).

The added resistance was finally estimated using the expression in equation 10.

$$R_{AW} = R_{Wave} - R_{Calm} \quad (10)$$

3. Results and Discussion

3.1 Resistance of the VLCC in Calm Water

The result for the VLCC's calm water resistance at 15, 17, and 20m draft are compared in Figure 2.

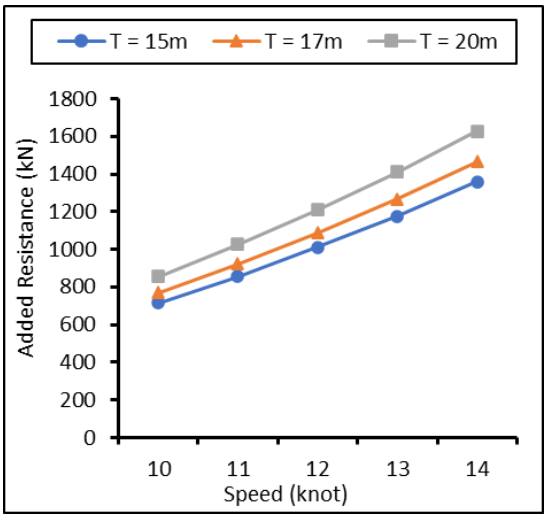

Figure 2: Calm Water Resistance of Very Large Crude-Oil Carrier at Varying Speeds and Drafts.

As observed in Figure 2, calm water resistance increased with increasing speed and draft. With an increase in draft, a higher frictional resistance is expected due to the greater area of the hull in contact with the water. The results show no significant increase in resistance in both scenarios, with that of draft indicating an increment range of 7.7 to 7.9% at the same speed while that of speed indicating an increment range of 33 to 37% at the same draft. These results are used as a basis to obtain the added resistance due to induced wave forces.

3.2 Added Resistance due to GoG's Wave Characteristics

To obtain the added resistance, the wave characteristics were computed in the MAXSURF motions module. The results illustrate the relationship between added resistance, draft, and wave period (Figure 3). As can be observed in Figure 3, the added resistance due to head waves decreased with speed, contrary to the conventional understanding that added resistance increases with speed. This may be explained by the fact that as the vessel speed increases, the relative motion between the ship and the waves changes. Higher speeds can result in less unfavorable wave impacts because the vessel may navigate through wave crests and troughs more quickly, thereby experiencing reduced resistance. Also, at higher speeds, the hull might achieve a planning effect, where the interaction with the waves becomes less severe due to a quicker distribution of wave effects over a larger area of the hull.

As illustrated in figure 4, the added resistance analysis demonstrated increase in resistance with longer wave periods across all drafts. This increase in added resistance with longer wave periods agrees with the fundamental interaction between the ship and the waves. Longer period waves carry more energy and have greater wavelengths, often approaching or exceeding the ship's length. This leads to more significant heaving and pitching motions of the vessel. Results also reveal that added resistance decreases with increasing draft. The deeper hull reduces the exposure of the vessel's bow to wave crests, thus mitigating the added resistance from wave impacts.

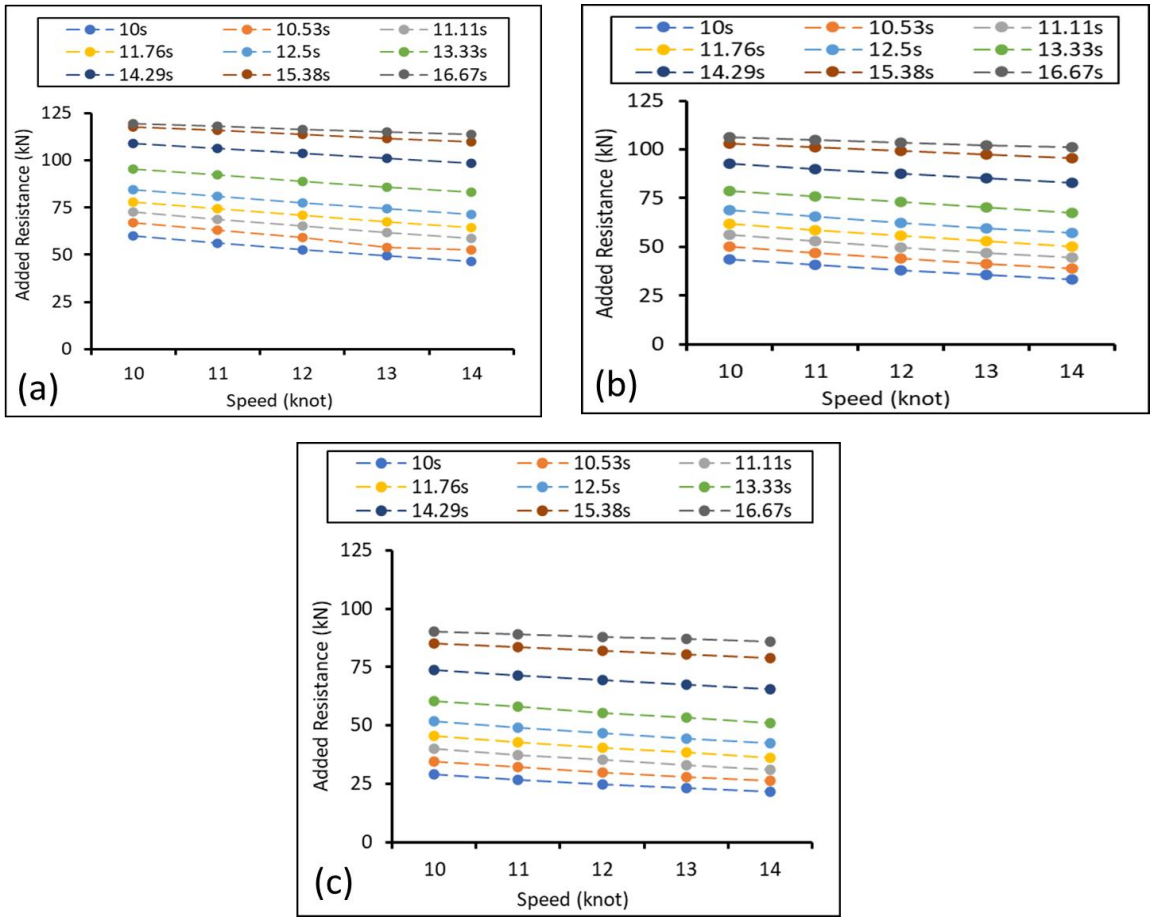

Figure 3: Added Resistance at (a) 15m Draft, (b) 17m Draft, and (c) 20m Draft.

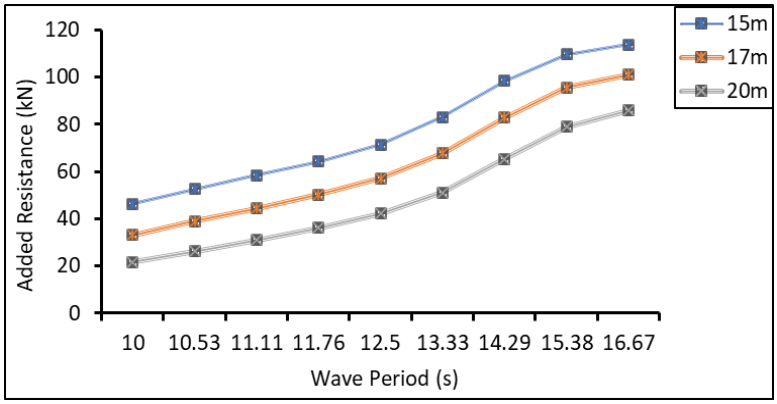

Figure 4: Effect of Wave Period on the Added Resistance

3.3 RAOs of the VLCC at 15m Draft

The RAOs for the VLCC at 15m draft, illustrated in Figure 5, was analyzed to provide critical insights into the vessel's behaviour in head and oblique seas. At 180° heading angle, the heave RAO begins at 0.83 at a wave frequency of 0.30 rad/s and decreases progressively to 0.46 at 0.38 rad/s. This trend indicates that the vessel experiences significant vertical motion in response to lower frequency waves, with the heave response decreasing as the wave frequency increases. The roll RAO remains at

0.00 across all frequencies, reflecting the absence of transverse instability of the vessel in head seas. The pitch RAO starts at 0.51 at 0.30 rad/s and gradually decreases to 0.33 at 0.38 rad/s. This behavior indicates that the vessel's bow and stern experience noticeable pitching motion, particularly at lower wave frequencies. The reduction in pitch RAO with increasing frequency is indicative of the vessel's hydrodynamic response to shorter waves, where the pitching motion becomes less significant.

The RAOs for a VLCC at 190-degree heading angle, analyzed at the vessel's center of gravity (CG), provide valuable insights into the ship's hydrodynamic response when subjected to waves approaching slightly off the bow. The heave RAO begins at 0.98 at a wave frequency of 0.21 rad/s and gradually decreases to 0.45 at 0.38 rad/s. This trend indicates that the vessel experiences significant vertical motions at lower frequencies, with the heave response decreasing as the wave frequency increases. The peak heave RAO of 0.98 suggests that the vessel is more prone to reactions at wave forces of a frequency of 0.21 rad/s, which could impact the comfort and safety of operations, particularly in extreme conditions where these forces are more pronounced. The roll RAO starts at 0.24 at 0.21 rad/s and peaks at 0.70 at 0.35 rad/s before decreasing to 0.54 at 0.38 rad/s. The peak roll RAO indicates that the vessel is most prone to rolling in these wave conditions, which could pose challenges to stability and comfort. The pitch RAO starts at 0.59 at 0.21 rad/s and decreases to 0.33 at 0.38 rad/s. The pitch RAO is higher at lower frequencies, reflecting the vessel's response to longer-period waves. As the wave frequency increases, the pitch RAO decreases, indicating reduced pitching motion in shorter-period waves. In the analysis of the RAOs for the VLCC at 201-degree heading angle, heave RAO starts at 0.98 and decreases to 0.49 as frequency increases, indicating a similar response to that of 190-degree. Roll RAO peaks at 1.44 at 0.36 rad/s, while pitch RAO starts at 0.55 and decreases to 0.32 as frequency increases.

3.4 RAOs of the VLCC at 17m Draft

As demonstrated in Figure 6, heave RAO begins at 0.98 at low frequencies at a heading angle of 180-degree and decreases steadily to 0.45 as frequency increases. Roll RAO is consistently zero, as expected for head-on waves while Pitch RAO begins at 0.60 and decreases to 0.34 with increasing frequency. At 190-degree heading angle, the heave RAO behaves similarly to the 180-degree case. Roll RAO is introduced, peaking at 0.66 at 0.32 rad/s, indicating moderate rolling motion. Pitch RAO is slightly lower than in the 180-degree case but follows a similar decreasing pattern. In the 201-degree heading angle, heave RAO remains like previous cases. Roll RAO increases significantly, exceeding 1.0 at 0.30 rad/s and peaking at 1.37 at 0.33 rad/s, indicating substantial rolling motion. Pitch RAO is lower than in previous cases but follows a similar decreasing pattern. This draft condition shows a balance between stability and responsiveness, with roll motion being the most sensitive to changes in heading angle.

3.5 RAOs of the VLCC at 20m Draft

In head seas, the VLCC experiences significant heave and pitch motions, while roll motions are negligible. The heave RAO peaks at lower frequencies (around 0.21-0.25 rad/s) with values close to 1 and decreases as frequency increases. Pitch RAO, illustrated in Figure 7 shows a similar trend but with lower magnitudes, peaking at about 0.6 at low frequencies and decreasing with increasing frequency. For 190-degree heading angle, heave and pitch responses are like the head seas condition but slightly reduced. The introduction of roll motion is notable, with RAO values peaking at around 0.7 at 0.32 rad/s. This indicates a significant roll response at this frequency. At a heading angle of 120-degree, heave responses remain like previous conditions. However, roll motion becomes much more significant, with RAO values exceeding 1 at frequencies around 0.29 to 0.33 rad/s, peaking at 1.44. Pitch response is slightly reduced compared to head seas but still considerable.

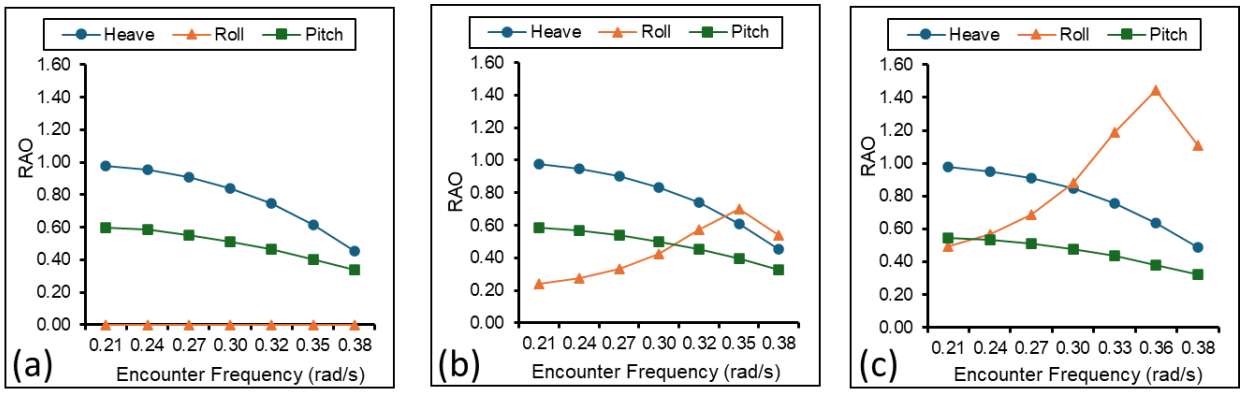

Figure 5: Response Amplitude Operators at 15m Draft at (a) 180° heading angle, (b) 190° oblique angle, and (c) 201° oblique angle.

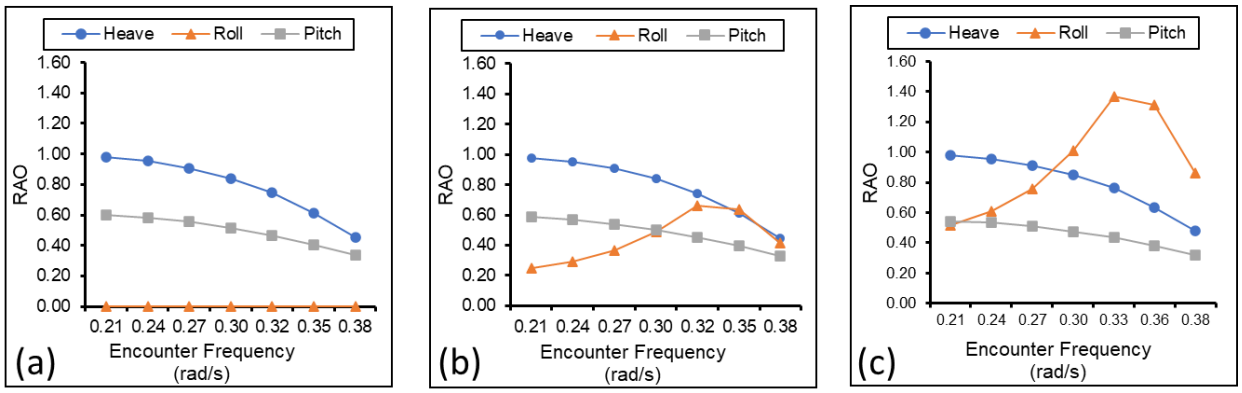

Figure 6: Response Amplitude Operators at 17m Draft at (a) 180° heading angle, (b) 190° oblique angle, and (c) 201° oblique angle.

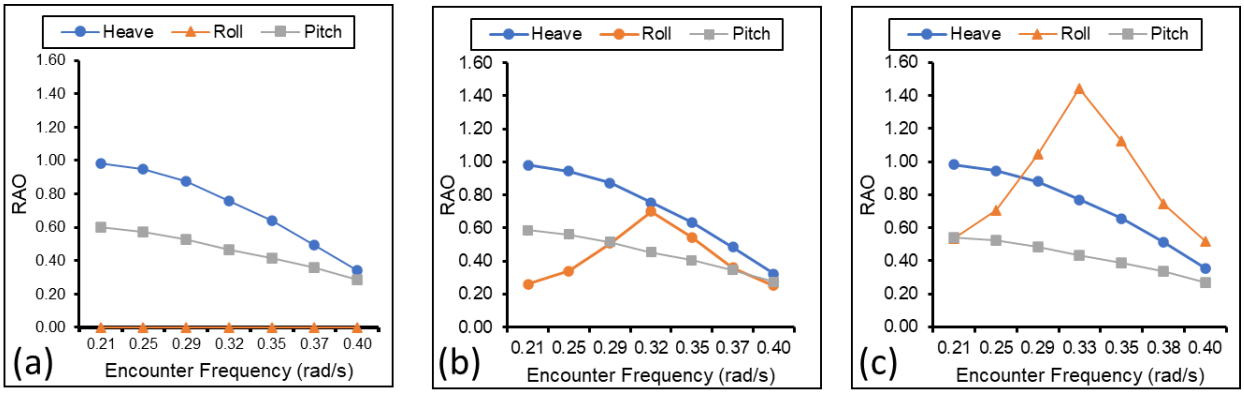

Figure 7: Response Amplitude Operators at 20m Draft at (a) 180° heading angle, (b) 190° oblique angle, and (c) 201° oblique angle.

4.0 Conclusions

This study effectively analyzed the calm water resistance, added resistance, and RAOs for a VLCC operating under typical Gulf of Guinea wave conditions. The calm water resistance results showed a clear increase with both vessel speed and draft, highlighting the impact of frictional forces as more hull surface interacts with water at deeper drafts and higher speeds. For added resistance in waves, results indicated that, contrary to conventional trends, added resistance decreased with increasing speed across all drafts. This was attributed to the potential reduction in wave impact duration at higher speeds, which may also introduce a partial planning effect, reducing the vessel's total resistance.

The RAO analysis across heave, roll, and pitch motions showed critical frequency ranges where each motion was most pronounced, with heave and pitch responses peaking in head seas (180° heading) and roll responses becoming significant in quartering seas (around 201°). Having established that the deeper drafts result in lower added resistance, the 17m draft was found to demonstrate a more stable roll response compared to the design draft of 20m, suggesting that 17m draft was enough submersion to dampen roll response to the wave forces. These findings contribute valuable insights into optimizing draft and operational speed for improved fuel efficiency and stability in the Gulf of Guinea, providing a foundation for enhanced operational planning and safety for VLCCs.

5.0 Recommendations

It is believed that the present semi-empirical modelling can predict the added resistance and motions of a VLCC in the Gulf of Guinea. However, there were certain limitations to the study, which would require further research. The following points highlight key areas for future research:

1. The use of MAXSURF modules, while effective, relies on certain assumptions and simplifications (e.g., linear wave theory and empirical formulas). These models may not fully capture complex, nonlinear interactions between the ship and waves, especially in extreme sea conditions. Future studies on this subject should apply more sophisticated approaches, that analyze the complex interactions between wave patterns, vessel dynamics, and environmental conditions.
2. The study focused primarily on the JONSWAP spectrum with the standard Peak Enhancement Factor of 3.3, as well as specific wave headings and heights. While this approach provides valuable insights, it is limited to moderate wave conditions of the region and might not fully cover the variability and complexity of the Gulf of Guinea region. More spectra should be used for similar research to compare and validate the results of this study.

Acknowledgements

Authors are grateful to all those who supported this research in the form of financial assistance and/or provision of the necessary resources.

References

Bai, Y., & Bai, Q. (2005). Subsea Pipelines and Risers. In Subsea Pipelines and Risers. https://doi.org/10.1016/B978-0-08-044566-3.X5000-3

Bertram, V. (2011). Practical Ship Hydrodynamics, Second Edition. In Practical Ship Hydrodynamics, Second Edition. https://doi.org/10.1016/C2010-0-68326-X

Birk, L. (2019). Fundamentals of Ship Hydro

dynamics. Fundamentals of Ship Hydro dynamics, 32. https://doi.org/10.1002/9781119191575

el Moctar, O., Sigmund, S., Ley, J., & Schellin, T. E. (2017). Numerical and experimental analysis of added resistance of ships in waves. Journal of Offshore Mechanics and Arctic Engineering, 139(1). https://doi.org/10.1115/1.4034205

Ibinabo, I., & Tamunodukobipi, D. T. (2019). Determination of the Response Amplitude Operator(s) of an FPSO. Engineering, 11(09), 541556. https://doi.org/10.4236/eng.2019.119038

ITTC. (2017). 28th ITTC Seakeeping Committee. November 2015.

Mazzaretto, O. M., Menéndez, M., & Lobeto, H. (2022). A global evaluation of the JONSWAP spectra suitability on coastal areas. Ocean Engineering, 266(P2), 112756. https://doi.org/10.1016/j.oceaneng.2022.112756

Niklas, K., & Karczewski, A. (2020). Determination of Seakeeping Performance for a Case. 27(108), 4–16.

Ouargli, H., & Hamoudi, B. (2021). Study of added resistance and seakeeping of KVLCC2 in waves with and without propeller. Ocean Systems Engineering, 11(2), 123–140. https://doi.org/10.12989/ose.2021.11.2.123

Petersson, E. (2002). Study of semi-empirical methods for ship resistance calculations. http://www.teknat.uu.se/student

Roser, A. P. (2018). Parametric Hull Form Variation and Assessment of Seakeeping Performance. Thesis- KTH Royal Institute of Technology.

Samson, N., & Adumene, S. (2015). Predictive Analysis of Bare-Hull Resistance of a 25 , 000 Dwt Tanker Vessel. 5(4), 194–198.

Seo, S., Park, S., & Koo, B. Y. (2017). Effect of wave periods on added resistance and motions of a ship in head sea simulations. Ocean Engineering, 137(March), 309–327. https://doi.org/10.1016/j.oceaneng.2017.04.009

Taskar, B., & Andersen, P. (2021). Comparison of added resistance methods using digital twin and full-scale data. Ocean Engineering, 229(January), 108710. https://doi.org/10.1016/j.oceaneng.2021.108710

Yan, X., Chen, C., & Fan, T. (2018). Effects of different wave spectra on dynamic positioning accuracy. Brodogradnja, 69(2), 83–92. https://doi.org/10.21278/brod69206

Zu, M., Garme, K., & Rosén, A. (2024). Seakeeping criteria revisited. Ocean Engineering, 297(December 2023). https://doi.org/10.1016/j.oceaneng.2024.116785